

*Citation for published version:*

Micallef, A, LeBas, TP, Huvenne, VAI, Blondel, P, Huenerbach, V & Deidun, A 2012, 'A multi-method approach for benthic habitat mapping of shallow coastal areas with high-resolution multibeam data', *Continental Shelf Research*, vol. 39-40, pp. 14-26. <https://doi.org/10.1016/j.csr.2012.03.008>

*DOI:*

[10.1016/j.csr.2012.03.008](https://doi.org/10.1016/j.csr.2012.03.008)

*Publication date:*

2012

*Document Version*

Peer reviewed version

[Link to publication](#)

NOTICE: this is the author's version of a work that was accepted for publication in *Continental Shelf Research*. Changes resulting from the publishing process, such as peer review, editing, corrections, structural formatting, and other quality control mechanisms may not be reflected in this document. Changes may have been made to this work since it was submitted for publication. A definitive version was subsequently published in *Continental Shelf Research*, vol 39-40, 2012, DOI: 10.1016/j.csr.2012.03.008

**University of Bath**

## **Alternative formats**

If you require this document in an alternative format, please contact:  
[openaccess@bath.ac.uk](mailto:openaccess@bath.ac.uk)

### **General rights**

Copyright and moral rights for the publications made accessible in the public portal are retained by the authors and/or other copyright owners and it is a condition of accessing publications that users recognise and abide by the legal requirements associated with these rights.

### **Take down policy**

If you believe that this document breaches copyright please contact us providing details, and we will remove access to the work immediately and investigate your claim.

Manuscript submitted to Continental Shelf Research:

**A multi-method approach for habitat mapping of the shallow coastal waters of the Maltese Islands with high-resolution multibeam data.**

Aaron Micallef <sup>a\*</sup>, Timothy P. Le Bas <sup>b</sup>, Veerle A.I. Huvenne <sup>b</sup>, Philippe Blondel <sup>c</sup>, Veit Hühnerbach <sup>b</sup> and Alan Deidun <sup>a</sup>

<sup>a</sup> University of Malta, Msida, MSD 2080, Malta.

<sup>b</sup> National Oceanography Centre, European Way, Southampton, SO14 3ZH, UK.

<sup>c</sup> Department of Physics, University of Bath, Bath, BA2 7AY, UK.

\*Corresponding author

E-mail: [aaron.micallef@um.edu.mt](mailto:aaron.micallef@um.edu.mt); Telephone: +356 99051124.

**ABSTRACT**

The coastal waters of the Maltese Islands, central Mediterranean Sea, sustain a diversity of marine habitats and support a wide range of human activities. The islands' shallow waters are characterised by a paucity of hydrographic and marine geo-environmental data, which is problematic in view of the requirements of the Maltese Islands to assess the state of their coastal waters by 2011 as part of the EU Marine Strategy Directive. Multibeam echosounder (MBES) systems are today recognised as one of the most effective tools to map the seafloor, although the quantitative characterisation of MBES data for seafloor and habitat mapping is still an underdeveloped field. The purpose of this

study is to outline a semi-automated, Geographic Information System-based methodology to map the distribution of seafloor composition and morphology in shallow coastal waters using high-resolution MBES data. We test this methodology in a 28 km<sup>2</sup> area of Maltese coastal waters. Three data sets were collected from this study area: (i) MBES bathymetry and backscatter data; (ii) Remotely Operated Vehicle imagery and (iii) photographs and sediment samples from dive surveys. Our approach combines a suite of topographic and textural analytical techniques to map different types of seafloor morphologies and compositions at various scales. Topographic analyses, based on bathymetric data, classify the seabed into five morphological zones and features – flat and sloping areas, crests, depressions and breaks of slope – by using morphometric attributes, the Bathymetric Position Index and geomorphometric mapping. Textural analyses of backscatter and bathymetry data segment the seafloor into four classes – medium sand, maerl associated with sand and gravel, seagrass settled on sand and gravel, and seagrass settled on bedrock - using roughness estimation, TexAn analyses and supervised classification based on information from training stations. The resulting topographic and seabed composition maps were combined to plot the distribution of the predominant habitats in the coastal waters offshore the NE Malta, some of which are of high conservation value. Ground-truthing of the habitat map using ROV imagery and dive observations confirms that our approach produces a simplified and accurate representation of seafloor habitats in a quick and objective manner while using all the information available within MBES data sets.

**Keywords:** habitat mapping; multibeam bathymetry; multibeam backscatter; coastal waters; Maltese Islands.

## 1. INTRODUCTION

Shallow coastal zones represent one of the most productive environments of the ocean and are characterised by complex mosaics of benthic habitats (Eyre and Maher, 2011; Gray, 1997). Knowledge of the spatial distribution, quality and quantity of these habitats is fundamental to our understanding of marine ecosystems and our ability to protect them from anthropogenic impacts (Jackson et al., 2001). Habitat maps have thus become a major tool in the assessment and monitoring of coastal marine systems, as well as in marine spatial planning, resource assessment and offshore engineering.

Historically, seafloor classification has largely been based on the collection of physical samples and divers' observations. In the last two decades, multibeam echosounder systems (MBES) have gained broad acceptance as a means to map large areas of the seafloor and delineate them into geological and geomorphological regions (Kostylev et al., 2001; Todd et al., 1999), to map the distribution of biological systems (Kostylev et al., 2003; McGonigle et al., 2009) and to identify archaeological components (Singh et al., 2000). The reasons for the increased popularity of MBES are numerous. First, MBES provide complete acoustic coverage of large swaths of the seafloor; in comparison, sampling and diving cover significantly smaller areas and are therefore less cost effective (Kenny et al., 2003). Second, recent developments in marine acoustic technology have allowed MBES to match or supersede other types of conventional acoustic survey systems (e.g. single beam echosounders, side scan sonar) as a mapping tool (Brown and Blondel, 2009). This is particularly the case for multibeam backscatter data, which today

1  
2  
3  
4 give as much, or more, detail than is available with side scan sonar systems alone (Le Bas  
5  
6 and Huvenne, 2009). The possibility of collecting bathymetric and backscatter data  
7  
8 simultaneously has thus led to a preference of MBES over side scan sonar as a marine  
9  
10 mapping tool (Brown et al., 2011).  
11  
12  
13  
14

15  
16 Seabed geology, in particular topography and composition, is known to influence benthic  
17  
18 community structure and ecological processes at many spatial scales (Bourget et al.,  
19  
20 1994; Cusson and Bourget, 1997; Guichard and Bourget, 1998; Kostylev et al., 2001;  
21  
22 Snelgrove and Butman, 1994) and is becoming an important component of seabed and  
23  
24 habitat mapping programs (e.g. Cochrane and Lafferty, 2002). Conventionally,  
25  
26 segmentation of MBES data sets into seabed geological features has been carried out  
27  
28 manually (e.g. Todd et al. (1999)). Manual segmentation is inherently subjective, slow  
29  
30 and potentially inaccurate (Cutter Jr. et al., 2003), which is problematic in view of the  
31  
32 subtle variations that may be present in acoustic responses, the large amount of data being  
33  
34 collected during modern surveys, and the increase in seabed mapping programmes  
35  
36 worldwide (Blondel and Gómez Sichi, 2009). There is thus a need to develop  
37  
38 quantitative, computational techniques that are robust, accurate and unbiased (Cutter Jr.  
39  
40 et al., 2003). These techniques should rapidly transform large areas of spatially-complex  
41  
42 bathymetric and backscatter data into simple, easily-visualised maps that supplement the  
43  
44 interpreter with as much information as possible. Mitchell and Clarke (1994) were among  
45  
46 the first to quantitatively characterise seabed geology using both bathymetric and  
47  
48 backscatter data. The quantitative classification of MBES data is an advancing field, and  
49  
50 several different approaches are currently under development and reported in the  
51  
52  
53  
54  
55  
56  
57  
58  
59  
60  
61  
62  
63  
64  
65

1  
2  
3  
4 literature (e.g. Erdey-Heydorn, 2008; Lamarche et al., 2011; Marsh and Brown, 2009;  
5  
6 Wright and Heyman, 2008).  
7  
8  
9

10  
11 The objectives of our study are to: (i) outline a quantitative, semi-automated method to  
12 map the distribution of seafloor composition and morphology; and (ii) to test the  
13  
14 applicability of this method in shallow coastal waters. We carry this out using high-  
15  
16 resolution multibeam bathymetry and backscatter data, together with precisely-geolocated  
17  
18 Remotely Operated Vehicle (ROV) imagery, dive observations and seabed samples,  
19  
20 acquired offshore the Maltese Islands, Mediterranean Sea.  
21  
22  
23  
24  
25  
26  
27

28  
29 Maltese coastal waters are characterised by a paucity of detailed hydrographic and marine  
30  
31 geo-environmental data. This is problematic in view of the requirement of the Maltese  
32  
33 Islands to carry out an initial assessment of the state of their coastal waters by 2011 as  
34  
35 part of the European Union Marine Strategy Directive. Considering that Maltese coastal  
36  
37 waters are also prone to various types of anthropogenic impacts, there is an urgent need  
38  
39 to develop tools for the rapid and accurate mapping of the Maltese seabed and to produce  
40  
41 good quality maps of its shallow seabed habitats.  
42  
43  
44  
45  
46  
47

## 48       **2.       REGIONAL SETTING**

49  
50  
51  
52

53 The Maltese archipelago is situated in the central Mediterranean Sea, between Italy and  
54  
55 North Africa, and consists of Malta, Gozo, Comino and a number of small uninhabited  
56  
57 islets (Figure 1a). The islands are composed of a series of Tertiary massive coralline  
58  
59  
60  
61  
62  
63  
64  
65

1  
2  
3  
4 limestones and fine-grained biomicrites with intercalated beds of phosphorite nodules and  
5  
6 clays (Pedley et al., 1976). This layered sequence is intensely disrupted by an Early  
7  
8 Miocene to mid-Pliocene NE-SW trending fault set, and a Late Pliocene NW-SE trending  
9  
10 fault system. The seabed around the Maltese Islands is one of the least studied areas in  
11  
12 Europe, although recent studies are showing that this region hosts important geological  
13  
14 (Micallef et al., 2011) and biological (Freiwald et al., 2009) systems. The Maltese Islands  
15  
16 are located at the south-western edge of the Malta Plateau, a shallow, north-south striking  
17  
18 ridge that links the Maltese Islands with Sicily (Figure 1a). The seabed topography  
19  
20 offshore the north-east of the Maltese Islands is generally shallow (mean depth of 115 m)  
21  
22 and gently sloping. The archipelago also straddles the northern rim of the Malta Graben,  
23  
24 a NW-SE oriented graben that has been active since the Late Miocene (Reuther and  
25  
26 Eisbacher, 1985). The seabed to the south-west of the Maltese Islands is thus steeper and  
27  
28 much deeper (>1000 m).  
29  
30  
31  
32  
33  
34  
35  
36  
37

## 38 FIGURE 1

39  
40  
41  
42 In this study we investigate a ~28 km<sup>2</sup> area of seabed located to the north-east of the  
43  
44 coastline of Malta, where the water depth varies between 6 and 57 m (Figure 1b). This  
45  
46 study area has been selected for two reasons. First, the area is known to host a variety of  
47  
48 seabed morphologies and substrate types (e.g. Borg et al., 2009; Sciberras et al., 2009),  
49  
50 making it an ideal site to assess the effectiveness of our technique. Secondly, the study  
51  
52 area falls within a Special Area of Conservation of International Importance  
53  
54 (MT0000105) under the EC Habitats Directive, which has been recently designated  
55  
56  
57  
58  
59  
60  
61  
62  
63  
64  
65

1  
2  
3  
4 within Maltese coastal waters to protect the extensive meadows of *Posidonia oceanica* (a  
5 seagrass species endemic to the Mediterranean Sea) located in the area. The study area is,  
6  
7 however, still prone to extensive human disturbance - it includes a popular tourist area  
8  
9 and dense urban settlements on shore, and busy recreational boating routes, vessel  
10  
11 bunkering zones, a fish farm and sites earmarked for a potential wind farm and  
12  
13 aquaculture zone offshore. The need to improve the spatial and environmental  
14  
15 management of the study area is thus urgent.  
16  
17  
18  
19  
20  
21  
22

### 23           **3.       DATA SETS**

24  
25  
26  
27  
28 Our study is based on three data sets acquired between October 2009 and August 2011.  
29  
30  
31  
32

33 The first data set was collected during a MBES survey aboard the R/V Hercules using a  
34 hull-mounted Kongsberg-Simrad EM-3002D system operating at a frequency of 300 kHz.  
35  
36 290 km of tracks were run at an average speed of 6.5 knots. The average swath width was  
37  
38 ~100 m, which allowed a swath overlap of 10-50% to be maintained. Positional data were  
39  
40 provided by a Trimble DSM 132 differential Global Positioning System (dGPS). Sound  
41  
42 velocity profiles were taken at the deepest point every day of the survey. Both bathymetry  
43  
44 and backscatter data were derived from the MBES survey (Figure 2). The bathymetry  
45  
46 data were processed with CARIS Hydrographic Information Processing System (HIPS)  
47  
48 by accounting for sound velocity variations, tides and basic quality control. The  
49  
50 backscatter data were processed with PRISM (Processing of Remotely-sensed Imagery  
51  
52 for Seafloor Mapping) software (Le Bas and Hühnerbach, 1998). Processing included  
53  
54  
55  
56  
57  
58  
59  
60  
61  
62  
63  
64  
65



radiometric corrections, geometric corrections and mosaicking. Bathymetric and backscatter data were exported as 32-bit rasters with a cell size of 1 m.

## FIGURE 2

The second data set includes underwater video surveys of ten seabed sites carried out from the R/V Hercules (Figure 2b). High-definition digital video imagery was acquired using a SeaEye Panther Plus Remotely Operated Vehicle (ROV) from a total area of 0.036 km<sup>2</sup> of seabed. Positional information was obtained from an Ultra-Short Baseline transponder relative to the ship's position.

The third data set consists of visual observations of main physical features and seabed composition, photographs and sediment samples obtained from seven sites during boat-based diving surveys (Figure 2b). Positional information was determined with buoys and dGPS. The sediment samples were collected using a small shovel and analysed for grain size distribution using a Coulter-Counter LS230 Laser Particle Size Analyser.

The ROV and diving sites were selected to encompass all the principal backscatter textures identified from the backscatter data. Dive sites A-F and ROV site G were used as training sites to ground-truth backscatter textures, whereas ROV sites 1-9 and dive site 10 were used as test sites to validate the results of our proposed methodology (Figure 2b).

## 4. METHOD AND RESULTS

Our methodological approach combines a suite of techniques that segment the acquired seabed data into habitats in terms of topographic and textural characteristics, generating information on both seabed physiography and composition (Figure 3). The method is thus divided into two types of analyses – topographical and textural analyses.

### FIGURE 3

#### 4.1 Topographic analyses

The goal of topographic analyses is to use the bathymetry data set to classify the seabed into five morphological zones and features – flat and sloping areas, crests, depressions and breaks of slope - which are the most elementary morphological units identified within the study area. To do this we employed three different morphometric methods (Figure 3).

##### 4.1.1 Flat and sloping areas

First, the study area was classified into flat and sloping zones. To characterise the general slope gradient of the seabed, we extracted the isobaths from the bathymetric data set at 2 m intervals, which we used to generate an interpolated surface. A slope gradient map, which is a measure of the maximum rate of elevation change from one cell to its neighbour, was then extracted from the interpolated surface  $3 \times 3$  cell neighbourhoods

using the ArcGIS™ Spatial Analyst extension. We used this method to determine the overall slope gradient of the seabed while ignoring the small-scale irregularities. The resulting map was then classified as flat (seabed with a slope gradient between 0° and 5°) or sloping (seabed with a slope gradient higher than 5°) (Figure 4a).

FIGURE 4

#### 4.1.2 Crests and depressions

The second step involved the extraction of crests and depression across the study area using the Bathymetric Position Index (BPI). BPI is a second-order derivative of bathymetry based on the Topographic Position Index (TPI) (Weiss, 2001), which was adapted for seafloor studies by Lundblad et al. (2006). The BPI algorithm uses a neighbourhood analysis function to evaluate the elevation differences between a focal point and the mean elevation of the surrounding cells within a user-defined shape. A negative BPI value represents a cell that is lower than its neighbouring cells (i.e. depression), whereas a positive value represents a cell that is higher (i.e. crest). Flat areas and areas of constant slope produce near-zero values. The BPI algorithm was implemented in ArcGIS™ using a raster calculator and the focal statistics mean tool (which calculates the mean value for a specified neighbour shape and size) on the bathymetric data set (Erdey-Heydorn, 2008). An annulus with an inner radius of 1 m and an outer radius of 5 m was used. Once the BPI data set was generated, the resulting map was reclassified in order to standardise the results to a mean of 0 and a standard deviation

of 100. This was carried out because bathymetry tends to be spatially auto-correlated (e.g. Goff et al., 2004; Malinverno, 1989), and the range of BPI values decreases with the radius of the annulus used. A standard deviation scheme was applied to extract crests (standardised BPI > 100) and depressions (standardized BPI < -100) from the BPI map (Figures 3 and 4b).

### 4.1.3 Breaks of slope

Certain morphological features of geological interest, such as faults, fissures and steep escarpments, consist of lineaments, discontinuities or boundaries that are not identified by zonal classifications. For this reason, we extracted a geomorphometric map of the study area to delineate breaks of slope (a change in slope gradient between adjacent cells that is higher than 60°) from a continuous grid of profile curvature. Profile curvature represents the change in slope gradient between adjacent cells. This attribute map was sliced into intervals of  $> 60^\circ \text{ m}^{-1}$  and  $< -60^\circ \text{ m}^{-1}$ , which were mapped as lineaments (Figure 4c). The methodology is described in more detail in Micallef et al. (2007).

## 4.2 Textural analyses

In sonar imagery classification, texture refers to the distribution of acoustic energy and their positions relative to each other (Blondel, 1996; Blondel and Gómez Sichi, 2009). Here we analyse the texture of the bathymetry and backscatter data to segment the seabed in terms of surficial composition.

#### 4.2.1 Ground-truthing

To characterise seabed composition we took into consideration the seabed photographs and sediment samples from the training sites (Figures 2b; 5). Sediment samples were divided into different classes according to their median grain size distribution ( $d_{50}$ ) and the Wentworth scale (Wentworth, 1922). We interpreted four main classes of seabed composition, in accordance with the marine habitats proposed for the Maltese Islands as aligned with the habitat classification system adopted within the EU Habitats Directive (Borg and Schembri, 2002). These classes include:

- (i) Medium sand (habitat III.3.3 Biocoenosis of coarse sands and muddy heterogeneous sediment);
- (ii) Maerl associated with sand and gravel (habitat III.3.2 Biocoenosis of coarse sand and fine gravels under the influence of bottom currents);
- (iii) Seagrass settled on sand and gravel (habitat III.5.1 Biocoenosis of *Posidonia oceanica* meadows; and
- (iv) Seagrass settled on bedrock (habitat III.5.1 Biocoenosis of *Posidonia oceanica* meadows).

These four classes are associated with characteristic backscatter intensities and textures at the seven training sites in Figure 5. The sand and gravel classes mainly comprised fragmented biogenic material, in particular carbonate shells. Maerl consists of accumulations of loose, living or dead, coralline algae (Bosence, 1979); since maerl beds

1  
2  
3  
4 serve as feeding ground for many species and are associated with high biodiversity levels,  
5  
6 they are listed in Annex V of the Habitats Directive as of community interest. The  
7  
8 *Posidonia oceanica* meadows are productive habitats that support a high diversity of  
9  
10 associated biota, and are listed as a priority natural habitat in Annex I of EC Directive  
11  
12 92/43/EEC on the Conservation of Natural Habitats and of Wild Fauna and Flora  
13  
14 (Hemminga and Duarte, 2000). The identified seagrass habitats predominantly included  
15  
16 matte, which is a hard surface of consolidated sand built up by *Posidonia oceanica* by  
17  
18 fixing carbonate as cement.  
19  
20  
21  
22  
23  
24  
25

26 FIGURE 5  
27  
28  
29  
30

#### 31 4.2.2 Estimation of roughness 32 33 34 35

36 Backscatter strength is a function of acoustic interactions with the seafloor, in particular  
37  
38 sediment grain size and roughness (Jackson and Richardson, 2007). Reducing the  
39  
40 influence of roughness on backscatter intensity facilitates classification of backscatter  
41  
42 data according to seabed composition. We carry this out by classifying the bathymetric  
43  
44 data from the study area in terms of seabed roughness and segmenting each zone  
45  
46 separately. We extracted a slope gradient map for  $3 \times 3$  cell neighbourhoods and  
47  
48 calculated the standard deviation of the slope gradient for  $3 \times 3$  cells, as proposed in  
49  
50 Micallef et al. (2007). Using this map, the seabed was divided into smooth and rough  
51  
52 zones according to a visually-selected threshold of 1 (Figure 6a).  
53  
54  
55  
56  
57  
58  
59  
60  
61  
62  
63  
64  
65

### 4.2.3 Classification

We utilised two different methods to classify the smooth and rough zones into seabed composition classes.

#### (a) Smooth zones: TexAn analyses and supervised classification

The training sites indicate that the smooth zone is predominantly comprised of unvegetated medium sand or maerl associated with sand and gravel. We segment the backscatter data in the smooth zone into these two classes using textural analyses.

Textural analyses quantitatively describe the grey levels and their spatial relationships in small windows throughout an image. Grey Level Co-occurrence Matrices (GLCMs) have been shown to be the most adaptable tools for textural analyses of sonar imagery (Blondel, 1996, 2000; Gao et al., 1998). GLCMs express the relative frequency of occurrence of two points at a certain Euclidean distance and angle from one another.

Three computation parameters – number of grey levels, the window size and the inter-pixel displacement – were required to calculate GLCMs. Textural indices were then used to describe the GLCMs resulting from these calculations. Two of these indices, entropy and homogeneity, are sufficient to resolve most textures visible in sonar imagery (Blondel, 1996; Blondel and Gómez Sichi, 2009; Blondel et al., 1998). Entropy measures the lack of spatial organisation inside the computation window, whereas homogeneity quantifies the amount of local similarities inside the computation window (Blondel, 1996). The optimal parameters were determined using backscatter textures for the classes

of medium sand and maerl associated with sand and gravel (Figure 5). Entropy and homogeneity indices were calculated for various values of grey levels numbers, window size and inter-pixel displacement. These parameters were then varied and the results plotted with backscatter intensity until the points for the classes of medium sand and maerl associated with sand and gravel were well separated in an entropy-homogeneity-backscatter graph (Figure 6b). This occurred when a minimum of 32 grey levels was used with a window size of  $50 \times 50$  pixels and an inter-pixel displacement of 10 pixels (Figure 6b). Maps of entropy and homogeneity were generated using these parameters. To ensure that the textural indices are not significantly influenced by the angle of ensonification, the co-occurrence matrices were averaged for angles of  $0^\circ$ ,  $45^\circ$ ,  $90^\circ$  and  $135^\circ$ , in accordance with Reed and Hussong (1989) and Blondel (1996). Classification signature files, storing the multivariate statistics for entropy, homogeneity and backscatter intensity, were generated for the two classes of sediment type using data from the training sites. A maximum-likelihood classifier, which uses a clustering algorithm to produce a grid of classes in the form of a raster thematic map, was used to assign each of the raster bands' to one of the classes in the signature file (Figure 6c). Textural analyses and supervised classification were respectively carried out using the software TexAn (Blondel, 2000) and ArcGIS<sup>TM</sup>.

FIGURE 6



## **(b) Rough zones: Morphometric attributes and supervised classification**

Rough zones consist predominantly of seagrass settled on sand and gravel, and seagrass settled on bedrock. We notice that the backscatter texture for these two classes of seabed composition does not differ significantly, which means that the seagrass cover contributes most to these textures, in agreement with observations by De Falco et al. (2010). This is expected at high multibeam frequencies, as used in this study, because they do not allow high penetration into the seabed. On the other hand, the distribution of seagrass seems to be directly influenced by the underlying substrate, resulting in discernibly different patterns in the bathymetry data set for seagrass settled on sand and gravel and seagrass settled on bedrock. Thus, we used bathymetric data to classify the rough zones into these two classes (Figure 3). First we derived morphometric maps of slope gradient and profile curvature from the bathymetric data. We then generated signature files from these two morphometric maps for the areas of seagrass settled on sand and gravel and seagrass settled on bedrock covered by the training sites. Based on these signature files, a maximum likelihood classification was carried out to generate the thematic map in Figure 6d.

### **4.3 Habitat mapping**

The resulting topographic and seabed composition maps (Figures 4a,b; 6c,d) were combined into a single habitat map using the Combine function in ArcGIS<sup>TM</sup>, which combines multiple rasters so that a unique output value is assigned to each unique

combination of input values. These maps were also slightly smoothed to eliminate small and isolated areas that do not translate well to actual habitat information and that are possibly misclassified. ArcGIS<sup>TM</sup> tools Boundary Clean (which cleans ragged edges between classes by shrinking and expanding them) and Majority Filter (which replaces cells in a raster based on the majority of their contiguous neighbouring cells) were used to carry out the smoothing. In this way, each cell in our study area was classified in terms of topography and seabed composition. The break of slope map (Figure 4c) was finally overlaid on the final habitat map (Figure 7).

FIGURE 7

## **5. DISCUSSION**

### **5.1 Shallow water habitats offshore NE Malta**

The predominant habitats offshore NE Malta are extents of medium sand, maerl associated with sand and gravel, seagrass settled on sand and gravel, and seagrass settled on bedrock, all located on flat areas (Figure 7). Other classes are considerably less abundant. The majority of the study area is covered by unvegetated medium sand, which is predominantly located in the southern half of the study area. The eastern boundaries of this habitat are characterised by an intricate pattern of lobes and ripples that are positive in relief and that are adjacent to, and occasionally cover, the maerl habitat (Figure 8b). We believe that these morphologies arise due to the influence of prevailing south-eastern

1  
2  
3  
4 flowing currents in the region (Drago et al., 2003), with the medium sand moving over  
5  
6 the maerl. The latter is prevalently interspersed with sand and gravel, and its coverage  
7  
8 includes the maerl grounds described by Borg et al. (1998). Maerl beds are known to  
9  
10 develop on level sea bottoms within the photic zone where waves or currents are strong  
11  
12 enough to turn over the free-living thalli, but not strong enough to break the brittle maerl  
13  
14 branches, such as open areas and sounds between islands (Steneck, 1986). The spatial  
15  
16 distribution of the maerl beds therefore provides an indication of the extent of seabed  
17  
18 affected by high velocity flows, associated with storm-induced bottom currents or  
19  
20 topographically-enhanced shallow water currents (Sciberras et al., 2009), or low  
21  
22 sedimentation rates.  
23  
24  
25  
26  
27  
28  
29  
30

## 31 FIGURE 8

32  
33  
34  
35

36 The seabed above ~40 m depth is largely dominated by different *Posidonia oceanica*  
37  
38 ecomorphoses. Most of the seagrass is settled on sand and gravel between Sikka l-Bajda  
39  
40 (a shallow, elongated, NW-SE trending limestone reef) and the NE coast of Malta (Figure  
41  
42 7). The rest of the seagrass is settled on bedrock; this habitat is mainly located in the  
43  
44 northern half of the study area on the Sikka l-Bajda reef, or close to the shoreline (Fra  
45  
46 Ben), where peninsulas have become submerged (Figure 7; 8c). The surface of the Sikka  
47  
48 l-Bajda reef is interrupted by circular to elliptical depressions with steep walls that are  
49  
50 filled with sand and gravel (Figure 8a). We identify four of these structures on the Sikka  
51  
52 l-Bajda reef and one on the Fra Ben peninsula to the south. The surface of Sikka l-Bajda  
53  
54 reef is also characterised by pockets of sand, gravel and maerl, which might have been  
55  
56  
57  
58  
59  
60  
61  
62  
63  
64  
65

preferentially deposited in bathymetric lows where the influence of wave action is reduced. The coverage of *Posidonia oceanica* meadows generally agrees with that mapped by Borg et al. (2009). The Sikka l-Bajda reef is fringed by a narrow band of sloping terrain, which is interrupted in places by gently sloping terraces and fault scarps. The latter are oriented NW-SE, in alignment with the active faults on shore.

## 5.2 Evaluation of method

An assessment of the predictive accuracy of the final habitat map comprises the best performance test for our method. We do this by visually comparing the ROV imagery and dive observations from the test sites, the locations of which are different from that of the training sites (Figure 2b), with the classes mapped in our habitat map (Figure 7).

For the most part, the mapped habitats coincide with the observations in the test sites (Figure 9). Misclassification of habitats and linear artefacts occur occasionally, particularly where data are characterised by noise or gaps, which is not surprising. Since flat areas cover >94% of the study area, our test sites only cover these areas and we are not able to assess the performance of the method for other types of morphologies from ROV and dive imagery. However, as shown in Figure 8, draping the habitat classes and breaks of slope on a 3D visualisation of the terrain shows that extracted elements coincide precisely with the features they are supposed to represent.

FIGURE 9

1  
2  
3  
4 We therefore consider that our approach has performed well overall. What distinguishes  
5  
6 our approach from previous methods is the fact that we use different techniques to map  
7  
8 different types of morphologies and composition at various scales. The selection of the  
9  
10 technique is based on identifying which geophysical parameter would be influenced by  
11  
12 the seabed type under consideration. The method requires minimal ground-truthing,  
13  
14 causes negligible disturbance to the seabed and does not require considerable computer  
15  
16 processing power. Our approach represents a substantial advantage over traditional  
17  
18 methods of data collection and interpretation used to map habitats offshore Malta – it  
19  
20 decreases the time and cost of data collection and interpretation, it reduces operator bias  
21  
22 and ensures consistency of classification results. The method is repeatable and can assess  
23  
24 evolution of the seabed over time, which has become a key factor in modern marine  
25  
26 environmental surveys. We manage to utilise all the information generated by the  
27  
28 multibeam sonar, which enhances the extraction and interpretation of topographic and  
29  
30 seabed information. The spatial detail of our mapping technique depends on the  
31  
32 resolution of the multibeam data set rather than the scale of observation, which ensures  
33  
34 that the maximum amount of information available from the data is obtained.  
35  
36  
37  
38  
39  
40  
41  
42  
43  
44

45 Backscatter data are shown to be an asset to seabed characterisation, and the quality of  
46  
47 the processed data is as good as those generated by side scan sonar. Our results confirm  
48  
49 that backscatter intensity can be used as a proxy for sediment grain size, in accordance  
50  
51 with Collier and Brown (2005) and Edwards et al. (2003). Principal Component Analysis  
52  
53 carried out for the backscatter, homogeneity and entropy data layers show that these  
54  
55 parameters explain 93.1%, 5.7% and 1.2% of sediment grain size variability, respectively,  
56  
57  
58  
59  
60  
61  
62  
63  
64  
65

1  
2  
3  
4 in Figure 6c. Excluding homogeneity and entropy from the supervised classification in  
5  
6 section 4.2.3 (b) results in higher noise and misclassification of habitats in some parts of  
7  
8 the map, in comparison to Figure 6c. Therefore, although backscatter is the main  
9  
10 characteristic determining segmentation of the study area into classes of medium sand  
11  
12 and maerl associated with sand and gravel, including texture parameters in the  
13  
14 classification improves the quality and reliability of backscatter classification, and the  
15  
16 final habitat map overall.  
17  
18  
19  
20  
21  
22

23  
24 Our method is semi-automated, and user input is still possible in the selection of the  
25  
26 decision boundaries to spatially separate classes, in choosing the data layers to input in  
27  
28 the classification technique and the classification method to be employed. Habitat  
29  
30 misclassifications and artefacts coincided with noise or gaps in the multibeam data  
31  
32 (Figure 9), and ideally these should be kept to a minimum during data collection. Other  
33  
34 limitations include the difficulty of discriminating between coarse sand and gravel from  
35  
36 maerl associated with sand and gravel (e.g. the maerl beds mapped across the Sikka l-  
37  
38 Bajda reef are likely to consist of sand and gravel only (Figure 7)), or between *Posidonia*  
39  
40 *oceanica* habitats with or without matte, due to the similar acoustic signature. The way to  
41  
42 take forward our work in the near future will therefore be to improve the method to  
43  
44 differentiate between different categories of the same habitat.  
45  
46  
47  
48  
49  
50  
51  
52  
53  
54  
55  
56  
57  
58  
59  
60  
61  
62  
63  
64  
65

## 6. CONCLUSIONS

The quantitative characterisation of MBES data for seafloor and habitat mapping is an advancing, but still underdeveloped, field that requires further research to realise the potential of the currently available MBES technology. In this study we demonstrate that the combination of high-resolution MBES bathymetry and backscatter data provides a robust means of producing detailed and accurate habitats maps of the shallow coastal waters of the Maltese Islands. Our approach consists of a semi-automated, GIS-based, multi-method system that combines a suite of topographic and textural analytical techniques to map different types of seafloor morphologies and composition at various scales. Topographic analyses, based on bathymetric data, classify the seabed into five morphological zones and features – flat and sloping areas, crests, depressions and breaks of slope – by using morphometric attributes, the Bathymetric Position Index and geomorphometric mapping. Textural analyses of backscatter and bathymetry data segment the seafloor into four classes of seabed composition – medium sand, maerl associated with sand and gravel, seagrass settled on sand and gravel, and seagrass settled on bedrock - using roughness estimation, TexAn analyses and supervised classification based on information from training stations. The resulting topographic and seabed composition maps were combined to plot the distribution of the predominant habitats in the coastal waters offshore NE Malta, some of which are of high conservation value. Ground-truthing of the habitat map by ROV imagery and dive observation confirms that our approach produces a simplified and accurate representation of seafloor habitats in a quick and objective manner, while using all the information available within MBES data

1  
2  
3  
4 sets. As the Government of Malta embarks on the mapping of its coastal waters in  
5  
6 fulfillment of its obligations under the Maritime Strategy Directive, we expect that our  
7  
8 approach can provide an efficient and cost-effective technique to map and manage  
9  
10 Maltese coastal waters.  
11  
12  
13  
14

## 15 16 **7. ACKNOWLEDGEMENTS** 17 18 19 20

21 This research was supported by grant 398 of the Royal Institution of Chartered Surveyors  
22  
23 (RICS) Education Trust and the University of Malta Research Fund 31-506. We kindly  
24  
25 acknowledge RPM Nautical Foundation, the captain and crew of R/V Hercules, and  
26  
27 Highland Geo Solutions for their assistance with data collection. Rut Pedrosa Pàmies is  
28  
29 thanked for her assistance with granulometric analyses. We are grateful to the  
30  
31 Hydrographic Office of the Malta Maritime Authority for providing access to bathymetric  
32  
33 data of the Maltese coastal waters. The ROV video and dive surveys were possible  
34  
35 following permits issued by the Environment Protection Directorate of the Malta  
36  
37 Environment and Planning Authority.  
38  
39  
40  
41  
42  
43  
44

## 45 46 **8. REFERENCES** 47 48 49

50 Blondel, P., 1996. Segmentation of the Mid-Atlantic Ridge south of the Azores, based on  
51  
52 acoustic classification of TOBI data, in: MacLeod, C.J., Tyler, P., Walker, C.L.  
53  
54 (Eds.), Tectonic, Magmatic and Biological Segmentation of Mid-Ocean Ridges.  
55  
56 Geological Society Special Publication, pp. 17-28.  
57  
58  
59  
60  
61  
62  
63  
64  
65



- 1  
2  
3  
4 Blondel, P., 2000. Automatic mine detection by textural analysis of COTS sidescan sonar  
5  
6 imagery. *International Journal of Remote Sensing* 21, 3115-3128.  
7  
8  
9 Blondel, P., Gómez Sichi, O., 2009. Textural analyses of multibeam sonar imagery from  
10  
11 Stanton Banks, Northern Ireland continental shelf. *Applied Acoustics* 70, 1288-  
12  
13 1297.  
14  
15  
16 Blondel, P., Parson, L.M., Robigou, V., 1998. TexAn: Textural analysis of sidescan sonar  
17  
18 imagery and generic seafloor characterisation, Oceans '98 IEEE/OES Conference  
19  
20 Proceedings, Nice, France, pp. 419-423.  
21  
22  
23 Borg, J.A., Howeg, H.M., Lanfranco, E., Micallef, S.A., Mifsud, C., Schembri, P.J.,  
24  
25 1998. The Macrobenthic Species of the Infralittoral to Circalittoral Transition Zone  
26  
27 off the Northeastern Coast of Malta (Central Mediterranean). *Xjenza* 3, 16-24.  
28  
29  
30 Borg, J.A., Rowden, A.A., Attrill, M.J., Schembri, P.J., Jones, M.B., 2009. Occurrence  
31  
32 and distribution of different bed types of seagrass *Posidonia oceanica* around the  
33  
34 Maltese Islands. *Mediterranean Marine Series* 10, 45-61.  
35  
36  
37 Borg, J.A., Schembri, P.J., 2002. Alignment of marine habitat data of the Maltese Islands  
38  
39 to conform to the requirements of the EU habitats directive (Council Directive  
40  
41 92/43/EEC), p. 136.  
42  
43  
44  
45 Bosence, D.W.J., 1979. Live and dead faunas from coralline gravels, Co. Galway.  
46  
47  
48 *Palaeontology* 22, 449-478.  
49  
50  
51 Bourget, E., DeGuise, J., Daigle, G., 1994. Scales of substratum heterogeneity, structural  
52  
53 complexity and the early establishment of a marine epibenthic community. *Journal*  
54  
55 *of Experimental Marine Biology and Ecology* 181, 31-51.  
56  
57  
58  
59  
60  
61  
62  
63  
64  
65

- 1  
2  
3  
4 Brown, C.J., Blondel, P., 2009. Developments in the application of multibeam sonar  
5  
6 backscatter for seafloor habitat mapping. *Applied Acoustics* 70, 1242-1247.  
7  
8  
9 Brown, C.J., Todd, B., J., Kostylev, V.E., Pickrill, R.A., 2011. Image-based classification  
10  
11 of multibeam sonar backscatter data for objective surficial sediment mapping of  
12  
13 Georges Bank, Canada. *Continental Shelf Research* 31, S110-S119.  
14  
15  
16 Cochrane, G.R., Lafferty, K.D., 2002. Use of acoustic classification of sidescan sonar  
17  
18 data for mapping benthic habitat in the Northern Channel Islands, California.  
19  
20  
21 Continental Shelf Research 22, 683-690.  
22  
23  
24 Collier, J.S., Brown, C.J., 2005. Correlation of sidescan backscatter with grain size  
25  
26 distribution of surficial seabed sediments. *Marine Geology* 214, 431-449.  
27  
28  
29 Cusson, M., Bourget, E., 1997. Influence of topographic heterogeneity and spatial scales  
30  
31 on the structure of the neighboring intertidal endobenthic macrofaunal community.  
32  
33  
34 Marine Ecology Progress Series 150, 181-193.  
35  
36 Cutter Jr., G.R., Rzhano, Y., Mayer, L.A., 2003. Automated segmentation of seafloor  
37  
38 bathymetry from multibeam echosounder data using local Fourier histogram texture  
39  
40 features. *Journal of Experimental Marine Biology and Ecology* 285-286, 355-370.  
41  
42  
43 De Falco, G., Tonielli, R., Di Martino, G., Innangi, S., Simeone, S., Parnum, I.M., 2010.  
44  
45 Relationship between multibeam backscatter, sediment grain size and *Posidonia*  
46  
47 *oceanica* seagrass distribution. *Continental Shelf Research* 30, 1941-1950.  
48  
49  
50 Drago, A.F., Sorgente, R., Ribotti, A., 2003. A high resolution hydrodynamic 3-D model  
51  
52 simulation of the Malta shelf area. *Annales Geophysicae* 21, 323-344.  
53  
54  
55  
56  
57  
58  
59  
60  
61  
62  
63  
64  
65

- 1  
2  
3  
4 Edwards, B.D., Dartnell, P., Chezar, H., 2003. Characterizing benthic substrates of Santa  
5  
6 Monica Bay with seafloor photography and multibeam sonar imagery. *Marine*  
7  
8 *Environmental Research* 56, 47-66.  
9  
10  
11 Erdey-Heydorn, M.D., 2008. An ArcGIS seabed characterization toolbox developed for  
12  
13 investigating benthic habitats. *Marine Geodesy* 31, 318-358.  
14  
15  
16 Eyre, B.D., Maher, D., 2011. Mapping ecosystem processes and function across shallow  
17  
18 seascapes. *Continental Shelf Research* 31, S162-S172.  
19  
20  
21 Freiwald, A., Beuck, L., Taviani, M., Hebbeln, D., R/V Meteor cruise M70-1  
22  
23 participants, 2009. The white coral community in the central Mediterranean Sea  
24  
25 revealed by ROV surveys. *Oceanography* 22, 58-74.  
26  
27  
28 Gao, D., Hurst, S.D., Karson, J.A., Delaney, J.R., Spiess, F.N., 1998. Computer-aided  
29  
30 interpretation of side-looking sonar images from the eastern intersection of the Mid-  
31  
32 Atlantic Ridge with the Kane Transform. *Journal of Geophysical Research* 103,  
33  
34 20997-21014.  
35  
36  
37  
38 Goff, J.A., Kraft, B.J., Mayer, L.A., Schock, S.G., Sommerfield, C.K., Olson, H.C.,  
39  
40 Gulick, S.P.S., Nordfjord, S., 2004. Seabed characterization on the New Jersey  
41  
42 middle and outer shelf: Correlatability and spatial variability of seafloor sediment  
43  
44 properties. *Marine Geology* 209, 147-172.  
45  
46  
47  
48 Gray, J.S., 1997. Marine biodiversity: Patterns, threats and conservation needs.  
49  
50 *Biodiversity and Conservation* 6, 153-175.  
51  
52  
53 Guichard, F., Bourget, E., 1998. Topographic heterogeneity, hydrodynamics and benthic  
54  
55 community structure: A scale-dependent cascade. *Marine Ecology Progress Series*  
56  
57 171, 59-70.  
58  
59  
60  
61  
62  
63  
64  
65

- Hemminga, M.A., Duarte, C.M., 2000. Seagrass Ecology. Cambridge University Press, Cambridge.
- Jackson, D.R., Richardson, M.D., 2007. High-Frequency Seafloor Acoustics. Springer, London.
- Jackson, J.B.C., Kirby, M.X., Berger, W.H., Bjorndal, K.A., Botsford, L.W., Bourque, B.J., Bradbury, R.H., Cooke, R., Erlandson, J., Estes, J.A., Hughes, T.P., Kidwell, S., Lange, C.B., Lenihan, H.S., Pandolfi, J.M., Peterson, C.H., Steneck, R.S., Tegner, M.J., Warner, R.R., 2001. Historical overfishing and the recent collapse of coastal ecosystems. *Science* 293, 629-638.
- Kenny, A.J., Cato, I., Desprez, M., Fader, G.B., Schuttenhelm, R.T.E., Side, J., 2003. An overview of seabed-mapping technologies in the context of marine habitat classification. *ICES Journal of Marine Science* 60, 411-418.
- Kostylev, V.E., Courtney, R.C., Robert, G., Todd, B., J., 2003. Stock evaluation of giant scallop (*Placopecten magellanicus*) using high-resolution acoustic for seabed mapping. *Fisheries Research* 60, 479-492.
- Kostylev, V.E., Todd, B., J., Fader, G.B., Courtney, R.C., Cameron, G.D., Pickrill, R.A., 2001. Benthic habitat mapping on the Scotian Shelf based on multibeam bathymetry, surficial geology and seafloor photographs. *Marine Ecology Progress Series* 219, 121-137.
- Lamarche, G., Lurton, X., Verdier, A.-L., Augustin, J.-M., 2011. Quantitative characterisation of seafloor substrate and bedforms using advanced processing of multibeam backscatter—Application to Cook Strait, New Zealand. *Continental Shelf Research* 31, S93-S109.

- 1  
2  
3  
4 Le Bas, T.P., Hühnerbach, V., 1998. PRISM Processing of remotely-sensed imagery for  
5  
6 seafloor mapping handbook. Southampton Oceanography Centre, p. 82.  
7  
8  
9 Le Bas, T.P., Huvenne, V.A.I., 2009. Acquisition and processing of backscatter data for  
10  
11 habitat mapping: Comparison of multibeam and sidescan systems. Applied  
12  
13 Acoustics 70, 1248-1257.  
14  
15  
16 Lundblad, E., Wright, D.J., Miller, J.P., Larkin, E.M., Rinehart, R., Battista, T.,  
17  
18 Anderson, S.M., Naar, D.F., Donahue, B.T., 2006. A benthic terrain classification  
19  
20 scheme for American Samoa. Marine Geodesy 29, 89-111.  
21  
22  
23 Malinverno, A., 1989. Testing linear models of seafloor topography. Pure and Applied  
24  
25 Geophysics 131, 139-155.  
26  
27  
28 Marsh, I., Brown, C., 2009. Neural network classification of multibeam backscatter and  
29  
30 bathymetry data from Stanton Bank (Area IV). Applied Acoustics 70, 1269-1276.  
31  
32  
33 McGonigle, C., Brown, C., Quinn, R., Grabowski, J., 2009. Evaluation of image-based  
34  
35 multibeam sonar backscatter classification for benthic habitat discrimination and  
36  
37 mapping at Stanton Banks, UK. Estuarine, Coastal and Shelf Science 81, 423-437.  
38  
39  
40 Micallef, A., Berndt, C., Debono, G., 2011. Fluid flow systems of the Malta Plateau,  
41  
42 Central Mediterranean Sea. Marine Geology 284, 74-85.  
43  
44  
45 Micallef, A., Berndt, C., Masson, D.G., Stow, D.A.V., 2007. A technique for the  
46  
47 morphological characterization of submarine landscapes as exemplified by debris  
48  
49 flows of the Storegga Slide. Journal of Geophysical Research 112, F02001.  
50  
51  
52 Mitchell, N.C., Clarke, J.E.H., 1994. Classification of seafloor geology using multibeam  
53  
54 sonar data from the Scotian Shelf. Marine Geology 121, 143-160.  
55  
56  
57  
58  
59  
60  
61  
62  
63  
64  
65

- Pedley, H.M., House, M.R., Waugh, B., 1976. The geology of Malta and Gozo. Proceedings of the Geologists' Association 87, 325-341.
- Reed, T.B., Hussong, D., 1989. Digital image processing techniques for enhancement and classification of SeaMARC II sidescan sonar imagery. Journal of Geophysical Research 94, 7469-7490.
- Reuther, C.D., Eisbacher, G.H., 1985. Pantelleria rift-crustal extension in a convergent intraplate setting. Geologische Rundschau 74, 585-597.
- Sciberras, M., Rizzo, M., Mifsud, J.R., Camilleri, K., Borg, J.A., Lanfranco, E., Schembri, P.J., 2009. Habitat structure and biological characteristics of a maerl bed off the northeastern coast of the Maltese Islands (central Mediterranean). Marine Biodiversity 39, 251-264.
- Singh, H., Adams, J., Mindell, D., Foley, D., 2000. Imaging underwater for archaeology. Journal of Field Archaeology 27, 319-328.
- Smith, W.H.F., Sandwell, D.T., 1997. Global seafloor topography from satellite altimetry and ship depth soundings. Science 277, 1957-1962.
- Snelgrove, P.V.R., Butman, C.A., 1994. Animal-sediment relationships revisited: Cause versus effects. Oceanography and Marine Biology Annual Review 32, 111-177.
- Steneck, R.S., 1986. The ecology of coralline algal crusts: Convergent patterns and adaptive strategies. Annual Review of Ecology and Systematics 17, 273-303.
- Todd, B.J., Fader, G.B.J., Courtney, R.C., Pickrill, R.A., 1999. Quaternary geology and surficial sediment processes: Browns Bank, Scotian Shelf, based on multibeam bathymetry. Marine Geology 162, 165-214.

Weiss, A.D., 2001. Topographic positions and landforms analysis, ESRI International User Conference, San Diego, California.

Wentworth, C.K., 1922. A scale of grade and class terms for clastic sediments. The Journal of Geology 30, 377-392.

Wright, D.J., Heyman, W.D., 2008. Introduction to the special issue: Marine and coastal GIS for geomorphology, habitat mapping and marine reserves. Marine Geodesy 31, 223-230.

## 9. FIGURE LEGENDS

Figure 1: (a) Bathymetric map of the central Mediterranean Sea showing the location of the Maltese Islands (isobaths at 50 m intervals; source: Smith and Sandwell (1997)); (b) Bathymetric map of the Maltese coastal waters (shallower than 100 m; isobaths at 10 m intervals), with the study area denoted by a black hatched polygon (source: Malta Maritime Authority; the bathymetric map should not be used for navigation purposes).

Figure 2: Processed (a) bathymetric data draped on a shaded relief map and (b) backscatter data, acquired from the study area. The location of the seven training sites and ten test sites are delineated in figure b.

Figure 3: Flowchart of the methodology used in this study. (BPI = Bathymetric Position Index (see section 4.1.2 for details); SSG = seagrass settled on sand and gravel; MSG = maerl associated with sand and gravel).

Figure 4: (a) Classification of study area into flat and sloping areas. (b) Enlarged section of the map of extracted crests and depressions, showing two irregular, channel-like features. (c) Enlarged section of the map of extracted breaks of slope. The locations of figures b and c are shown in figure a.

Figure 5: Backscatter imagery (200 m × 200 m) and description of backscatter textures at the seven training sites (locations shown in Figure 2b). High backscatter is represented by light colours, low backscatter by dark colours. A representative seabed photograph and the interpreted seabed composition (from seabed imagery and samples) are also included.

Figure 6: (a) Classification of bathymetric data into smooth and rough zones based on the standard deviation of slope gradient. (b) 3D feature space graph of medium sand (dark blue) and maerl associated with sand and gravel classes (light blue) in terms of backscatter, homogeneity and entropy. (c) Supervised classification map of smooth zones into medium sand and maerl associated with sand and gravel classes. (d) Supervised classification map of rough zones into 2 classes: seagrass settled on sand and gravel, and seagrass settled on bedrock. (MS = medium sand; MSG = maerl associated with sand and gravel; SSG = seagrass settled on sand and gravel; SB = seagrass settled on bedrock).

Figure 7: (a) Habitat map generated by combining the topographic and seabed composition maps; (b) Pie chart of the areal fraction of each habitat across the study area (numbers denote coverage in km<sup>2</sup>).



Figure 8: Habitat map draped on 3D DEM for three sections from the habitat map: (a) Circular bedrock depression infilled with medium sediment; (b) Intricate pattern of lobes and ripples of medium sand overlying maerl associated with sand and gravel; (c) Submerged bedrock peninsula covered with seagrass and bordered by seagrass settled on sand and gravel. The location of these sections is denoted in figure 7a.

Figure 9: Habitat description and predicted seabed composition (200 m × 200 m; legend shown in Figure 7), compared with ROV still imagery and interpreted seabed composition for test sites.

Figure 1  
[Click here to download high resolution image](#)

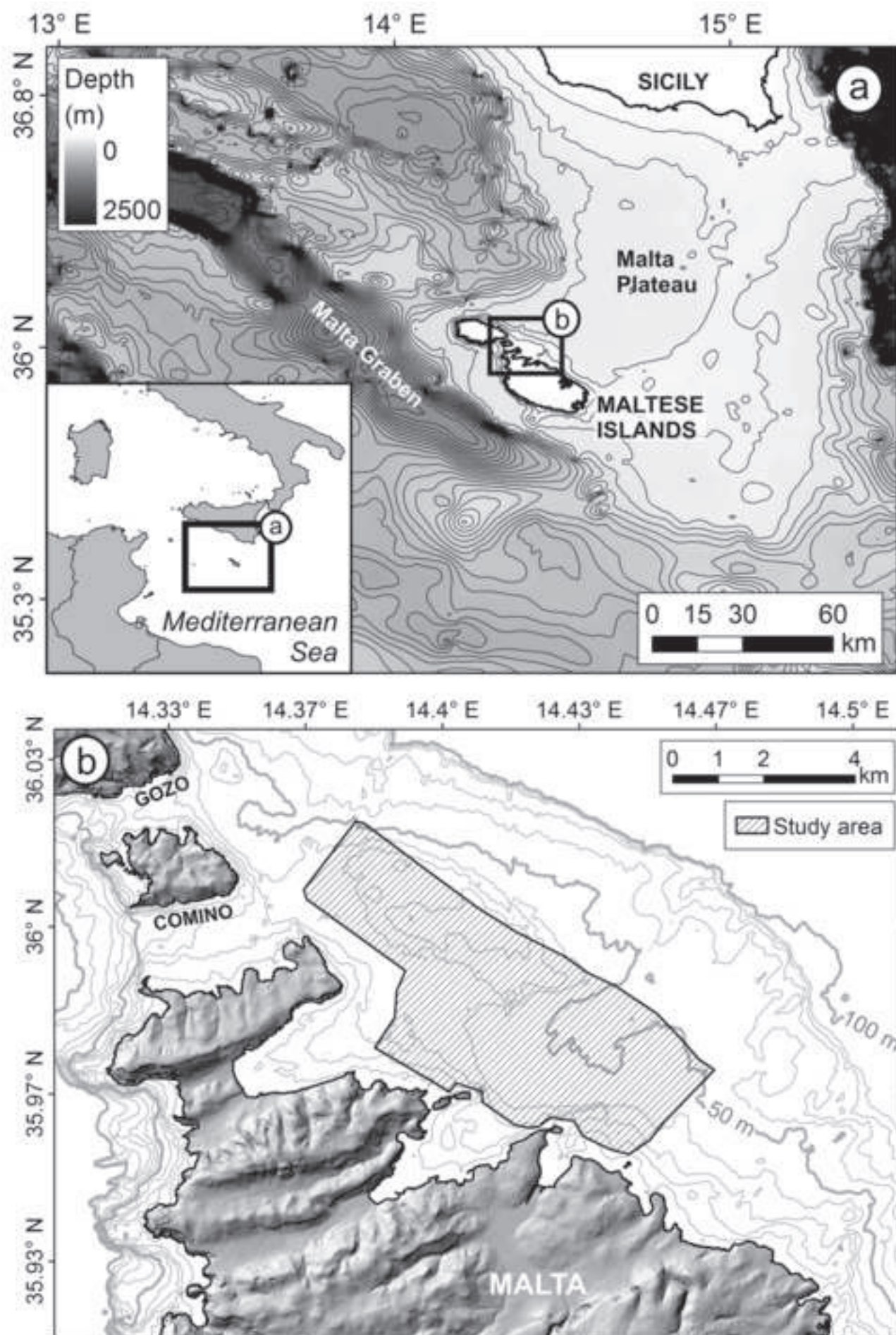


Figure 2  
[Click here to download high resolution image](#)

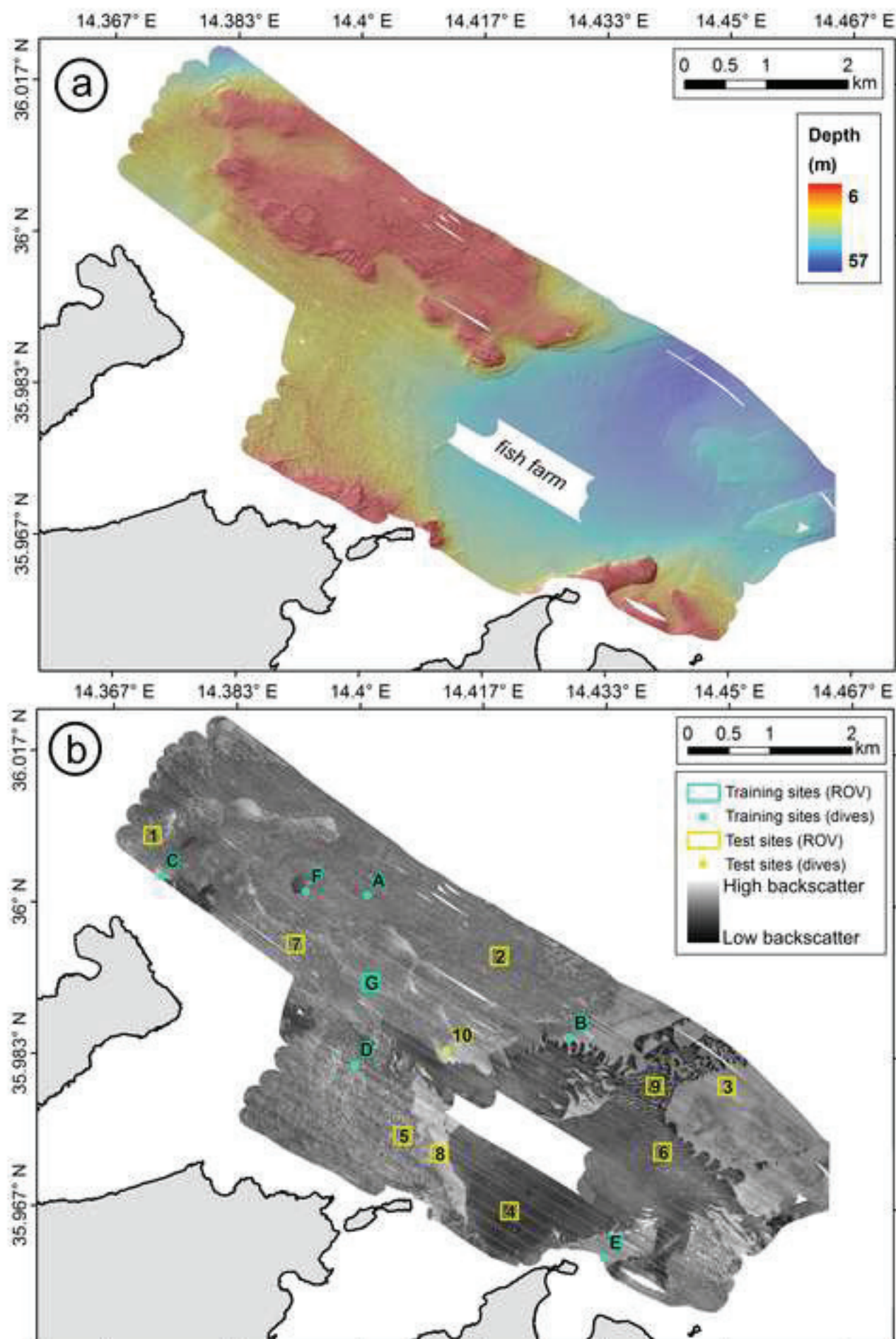




Figure 3  
[Click here to download high resolution image](#)

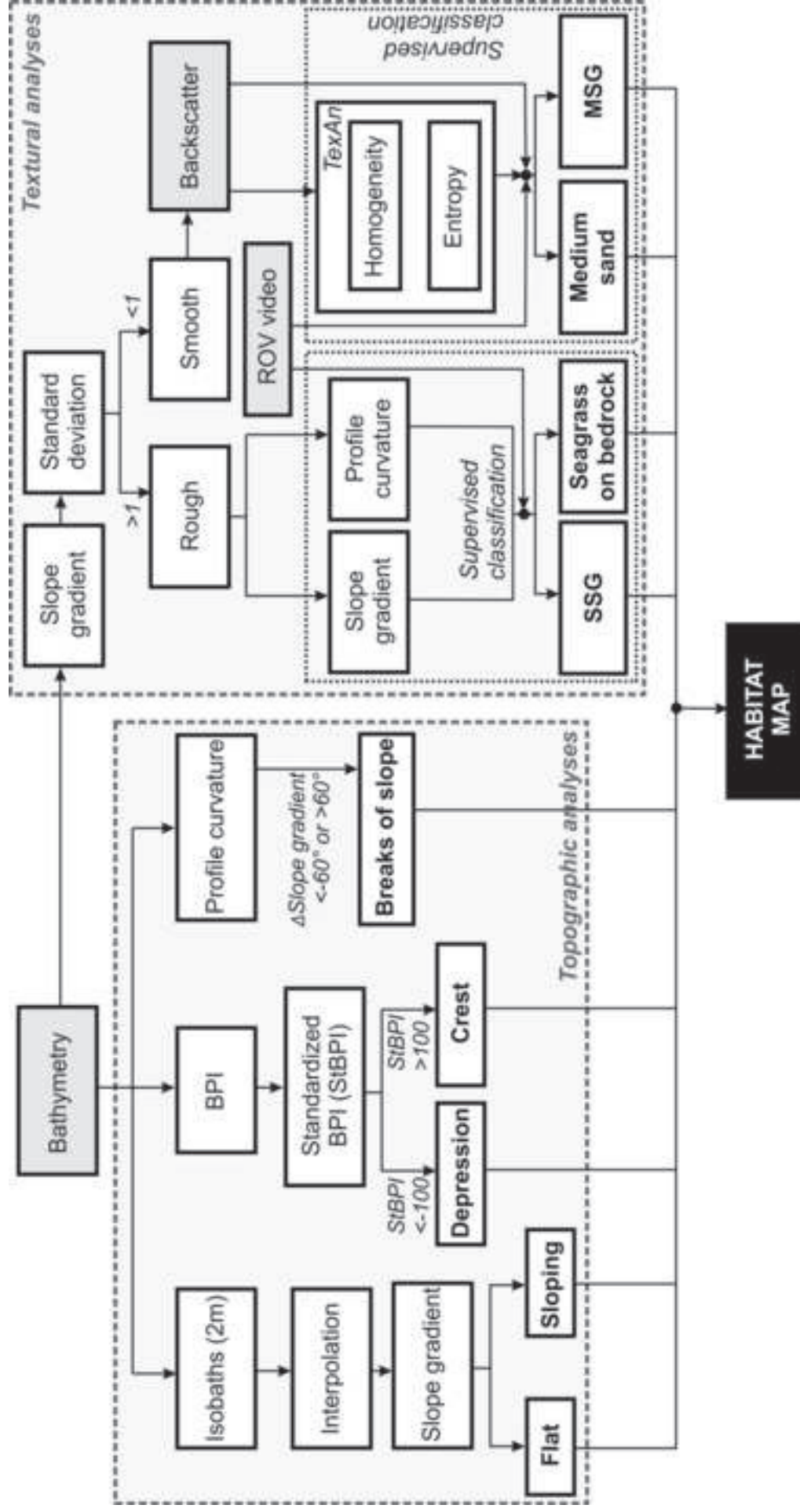
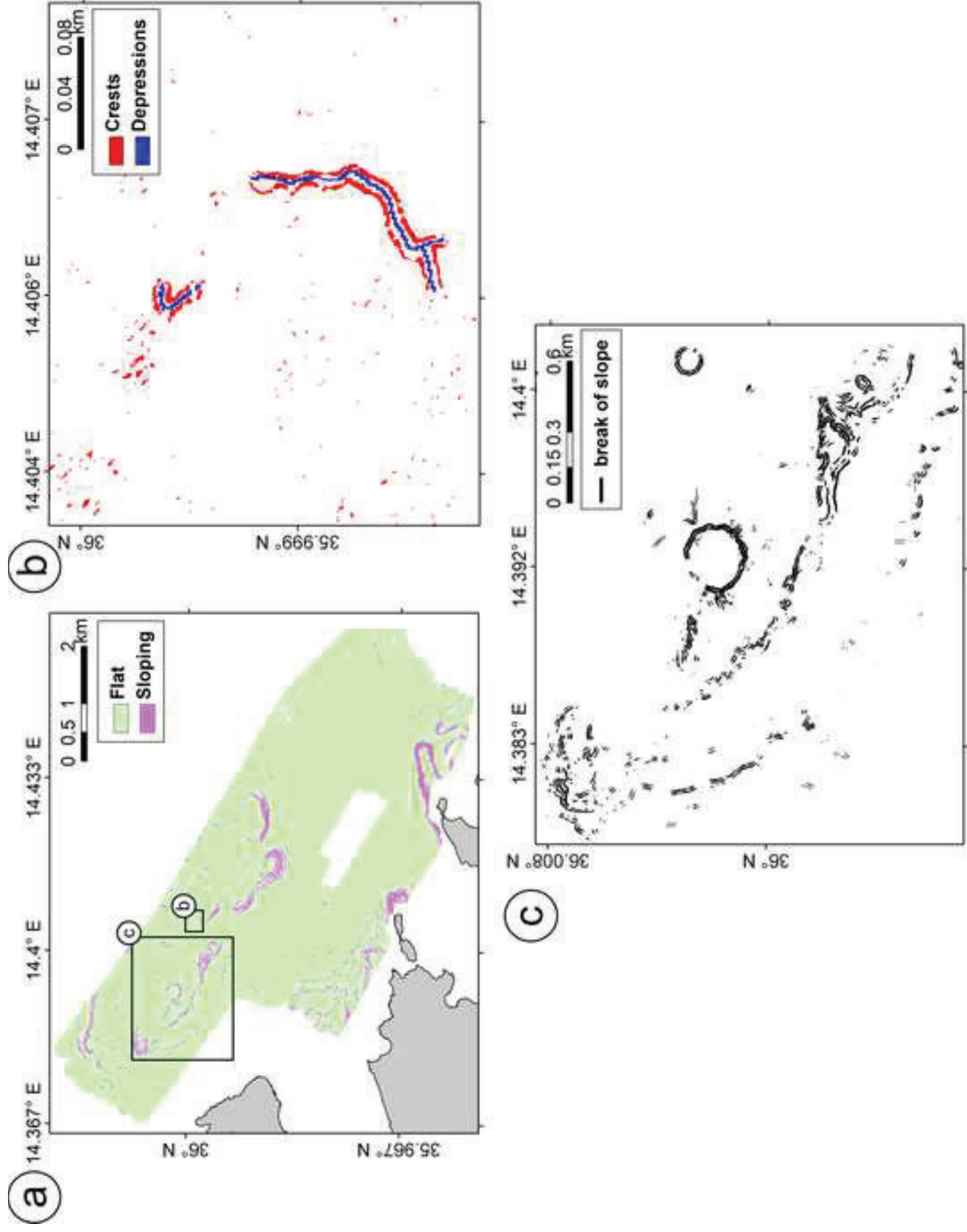


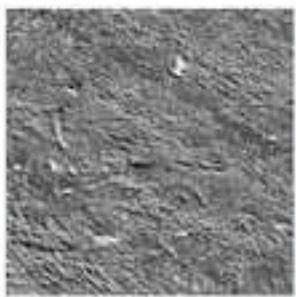
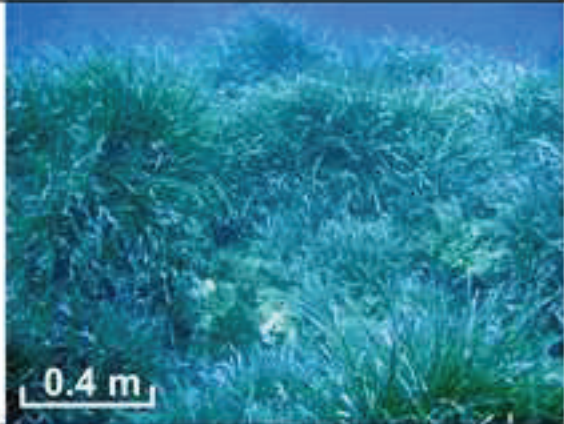

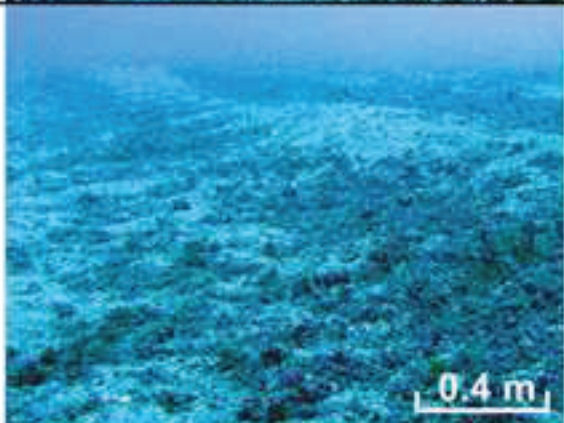

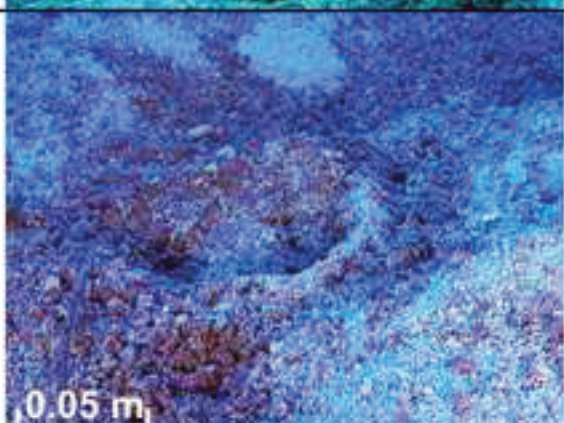
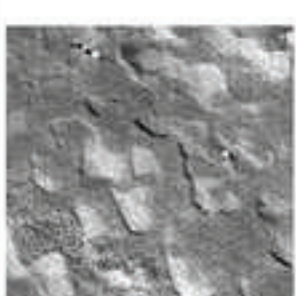

Figure 4

[Click here to download high resolution image](#)





**Figure 5**  
[Click here to download high resolution image](#)

Backscatter image and training site number	Texture description	Seabed image	Seabed composition
 <p>A</p>	Speckled pattern of intermediate backscatter		Bedrock covered by discontinuous seagrass cover
 <p>B</p>	Homogeneous pattern of high backscatter		Maerl interspersed with sand and gravel
 <p>C</p>	Homogeneous pattern of high backscatter		Maerl interspersed with sand and gravel
 <p>D</p>	Intermediate backscatter pattern interrupted by elongated patches of high backscatter		Superficially coarse sand to fine gravel covered by dense patches of seagrass



**Figure 5b**  
[Click here to download high resolution image](#)

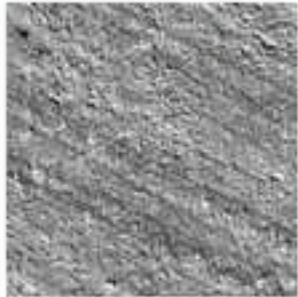
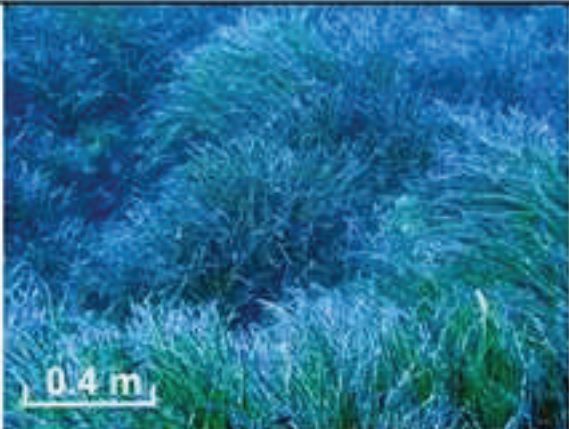
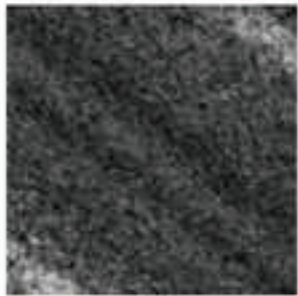
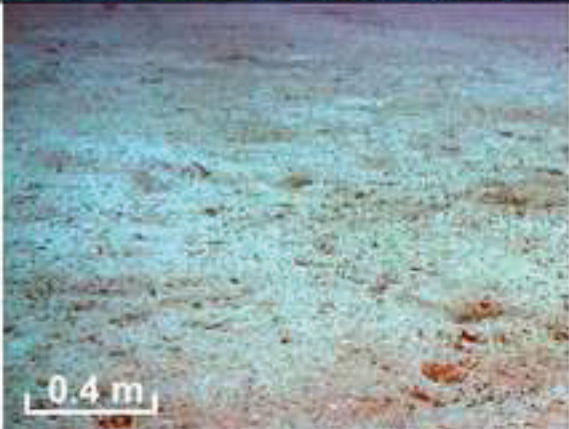
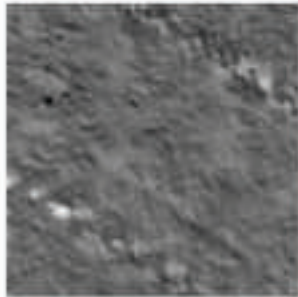

Backscatter image and training site number	Texture description	Seabed image	Seabed composition
 <p>E</p>	Speckled pattern of intermediate backscatter		Bedrock covered by dense seagrass cover
 <p>F</p>	Homogeneous pattern of low backscatter		Superficially medium sand
 <p>G</p>	Intermediate to low backscatter interrupted by an irregular pattern of intermediate backscatter		Superficially medium sand covered by dense patches of seagrass

Figure 6  
[Click here to download high resolution image](#)

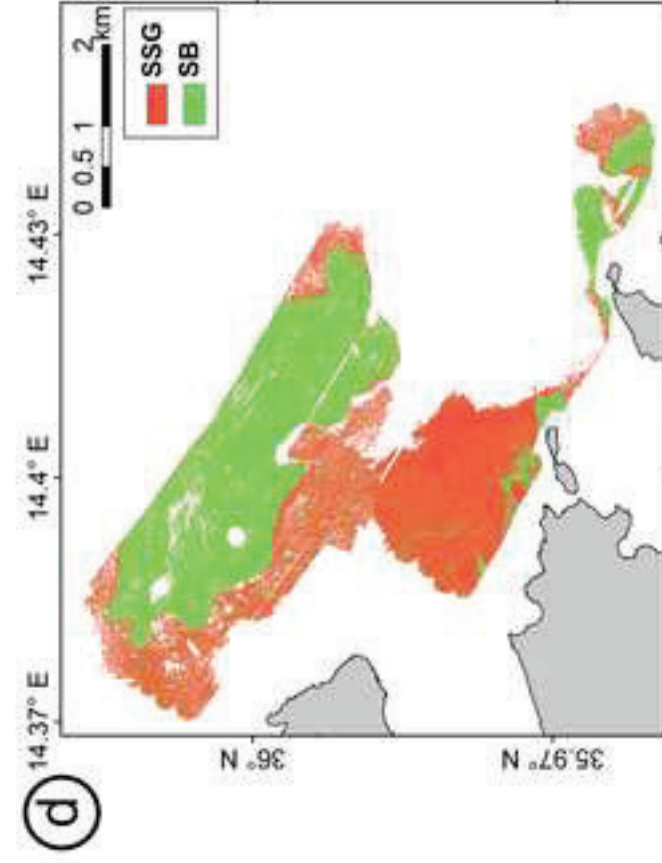
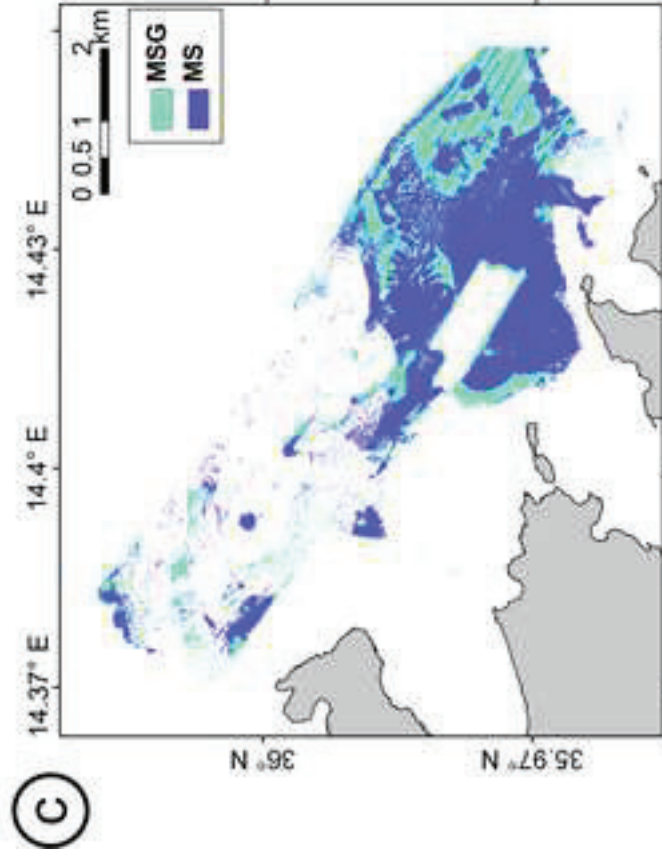
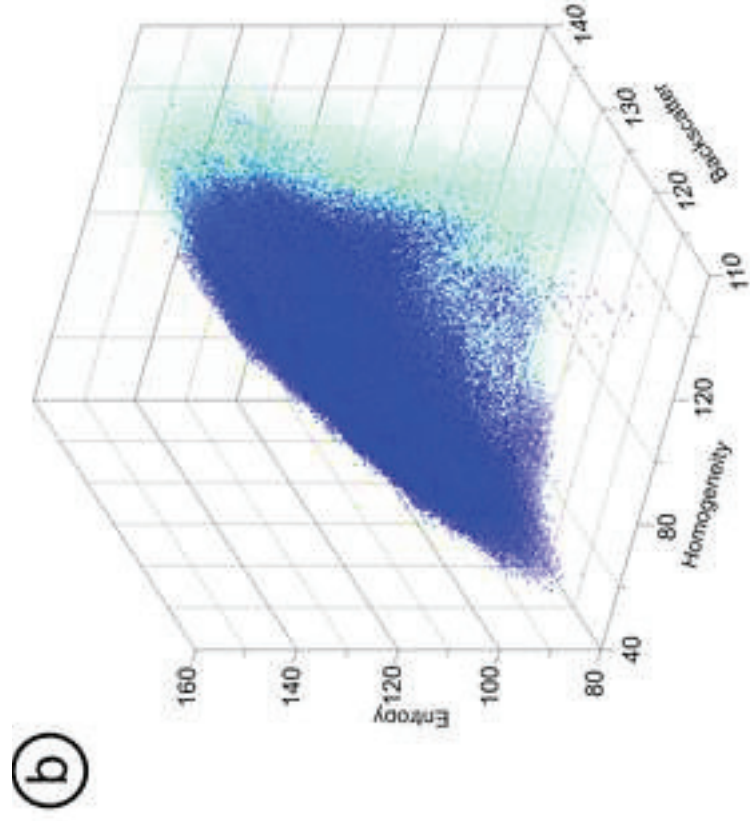
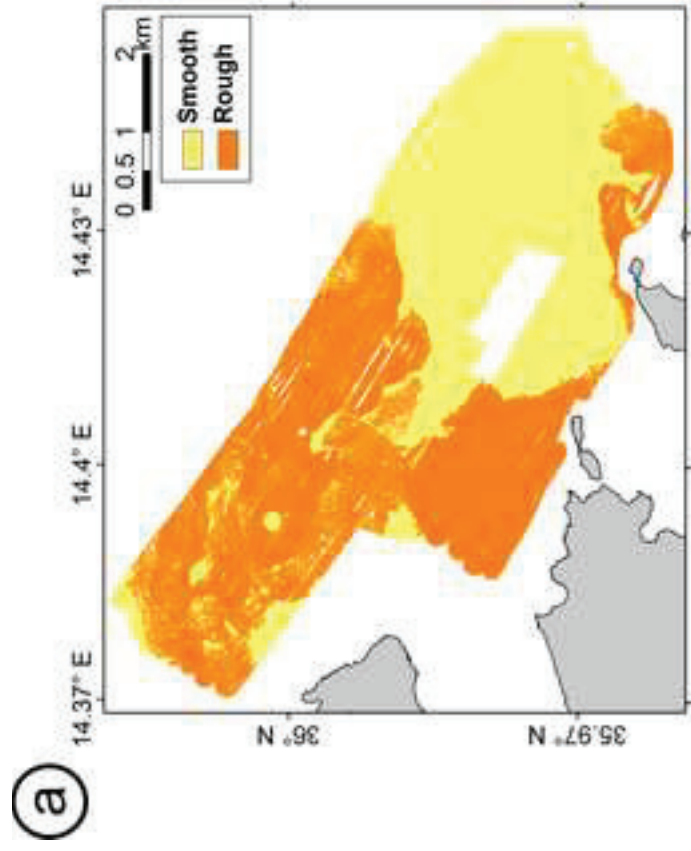




Figure 7  
[Click here to download high resolution image](#)

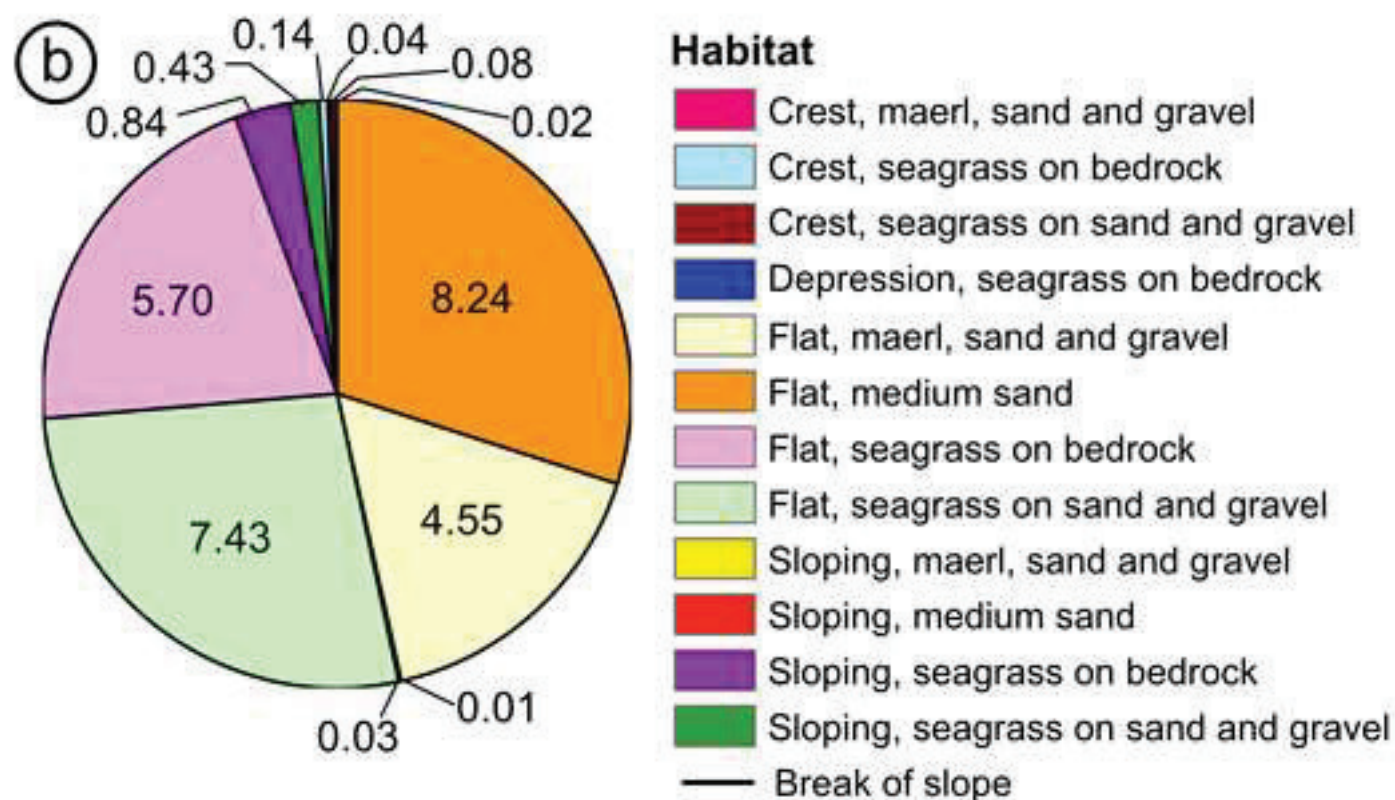
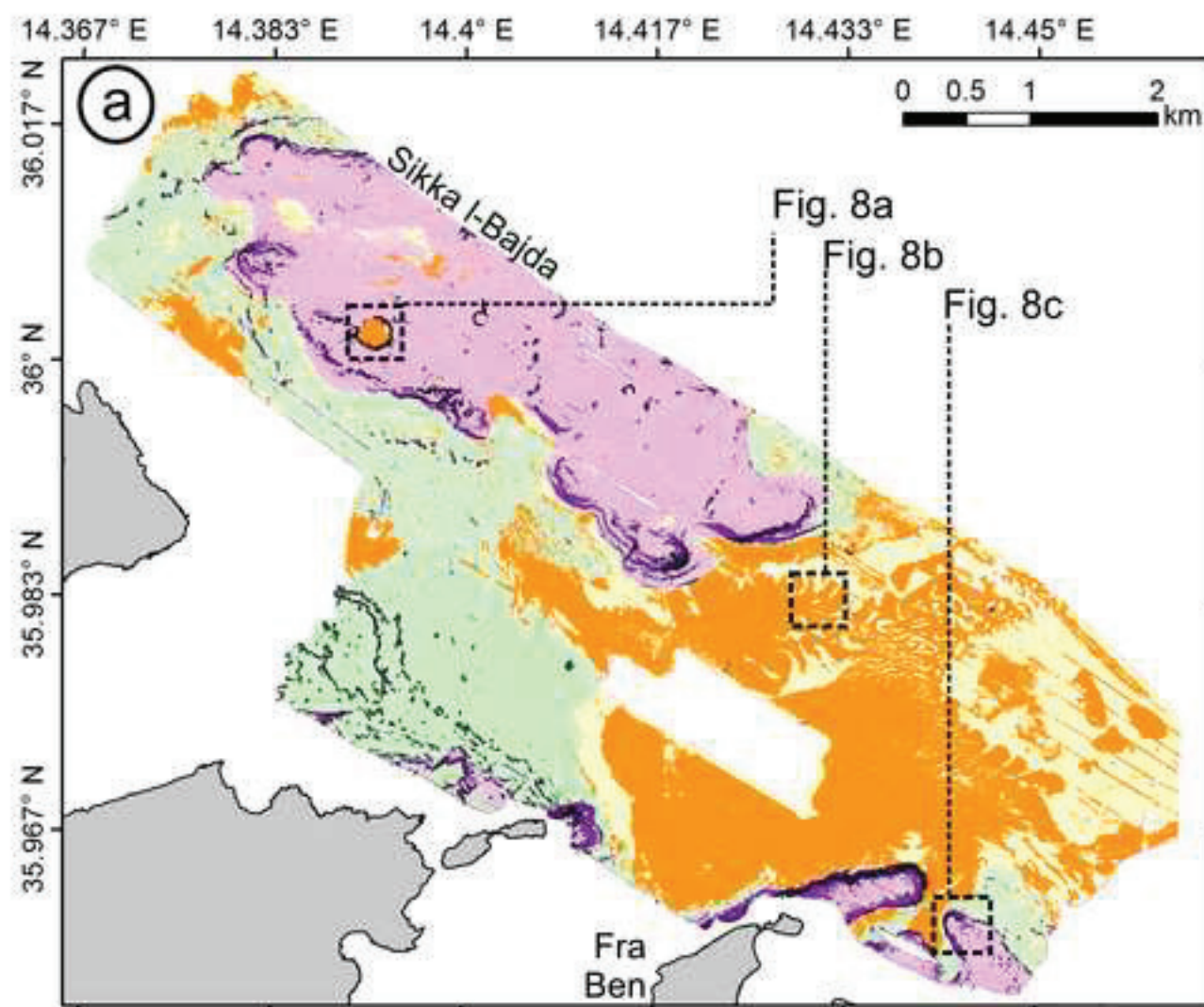
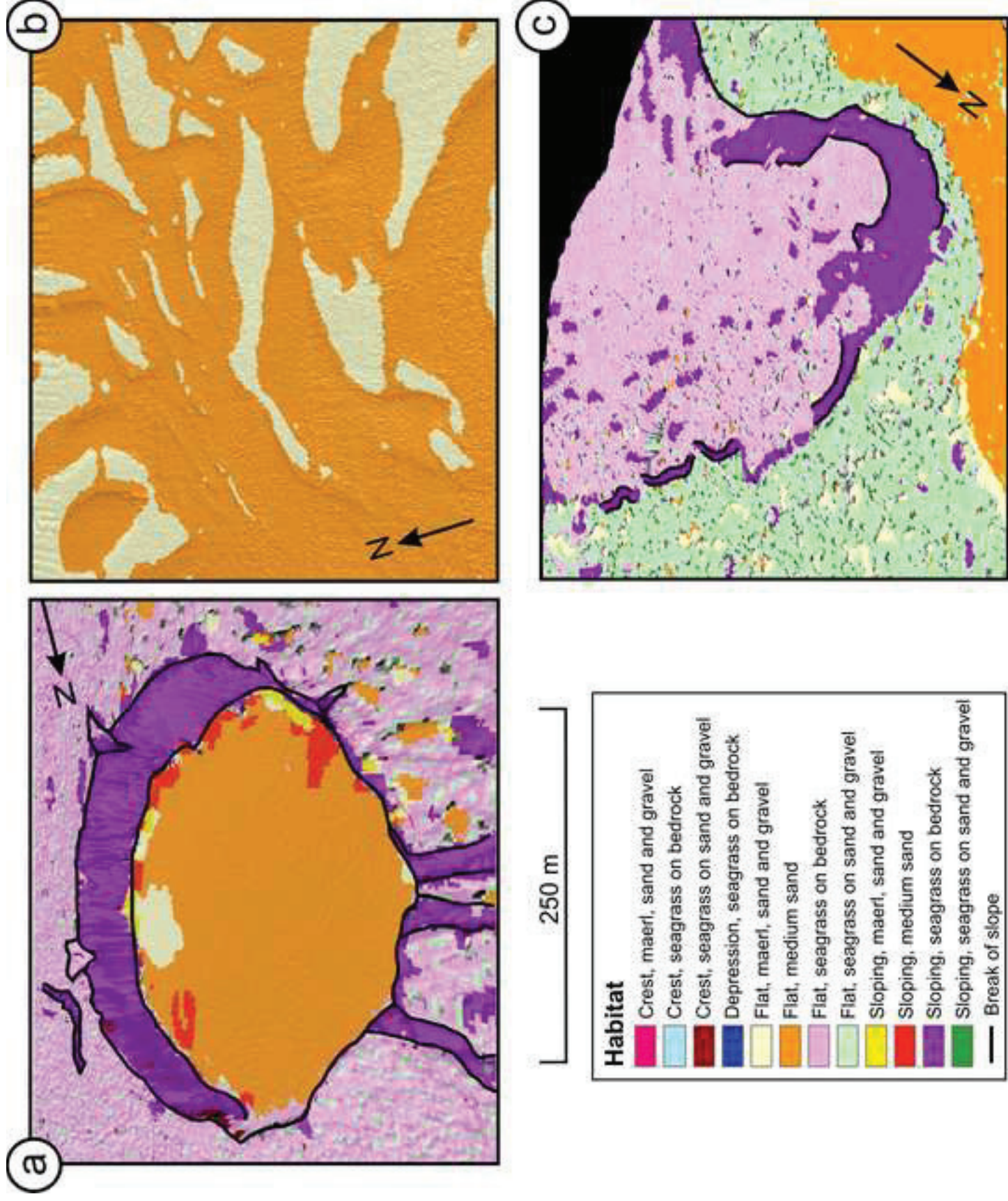




Figure 8  
[Click here to download high resolution image](#)





**Figure 9a**  
[Click here to download high resolution image](#)

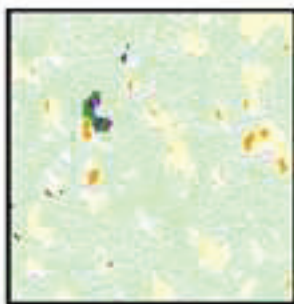
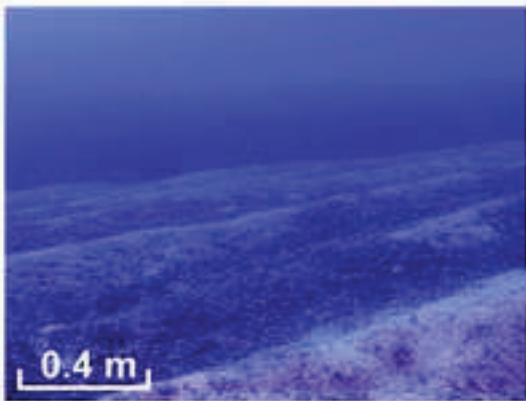
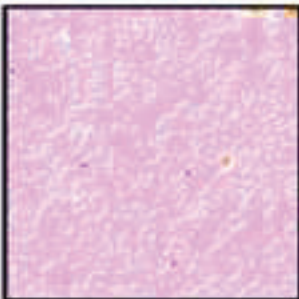
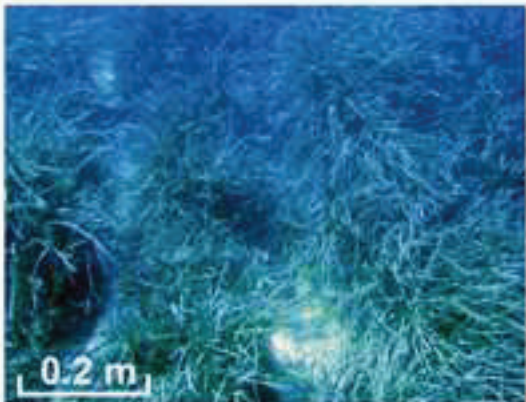
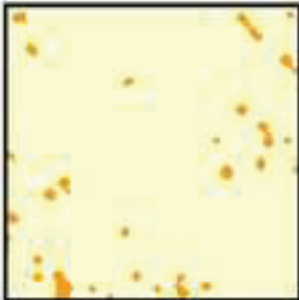
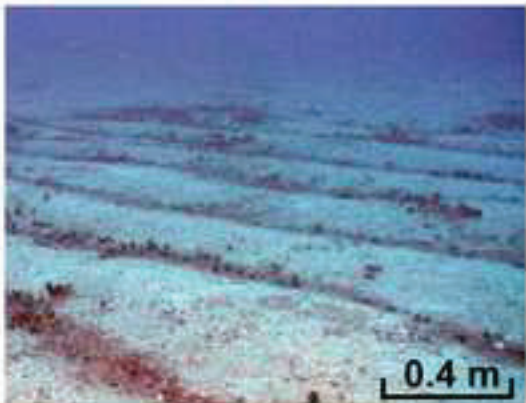

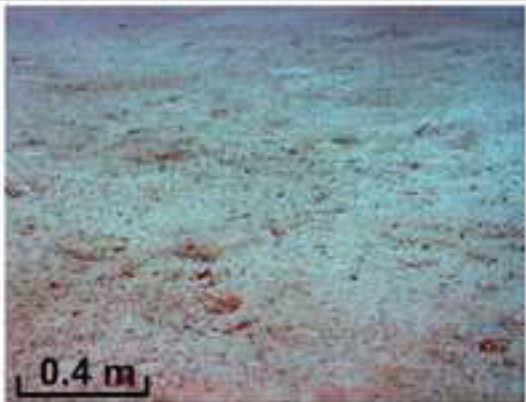
Test site	Predicted seabed composition	Seabed image	Seabed composition
 <p>1</p>	Seagrass on sand and gravel interrupted by patches of maerl associated with sand and gravel, flat		Seagrass meadow interrupted by patches of maerl associated with sand and gravel
 <p>2</p>	Seagrass on bedrock, flat		Bedrock covered by dense growth of seagrass
 <p>3</p>	Maerl associated with sand and gravel, flat		Maerl associated with sand and gravel
 <p>4</p>	Medium sand, flat		Superficially medium sand

Figure 9b

[Click here to download high resolution image](#)


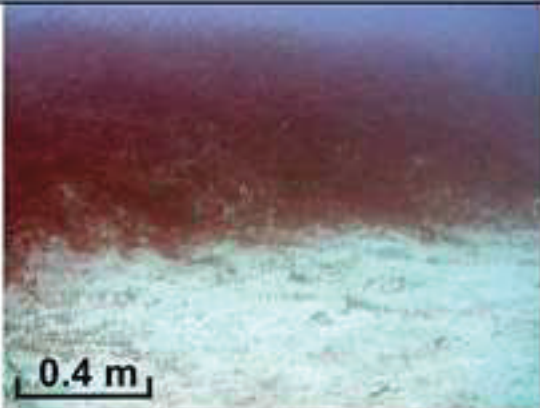
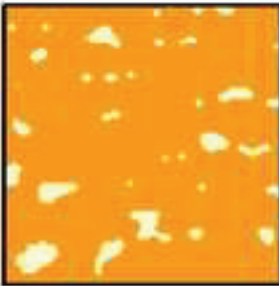
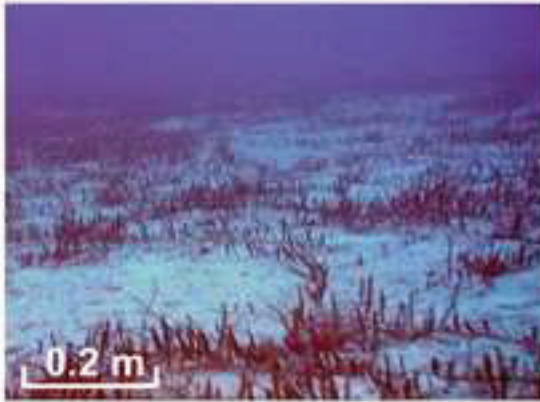
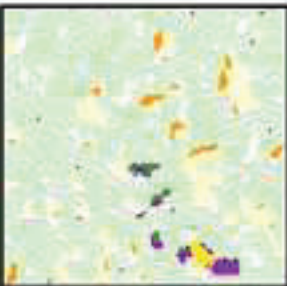
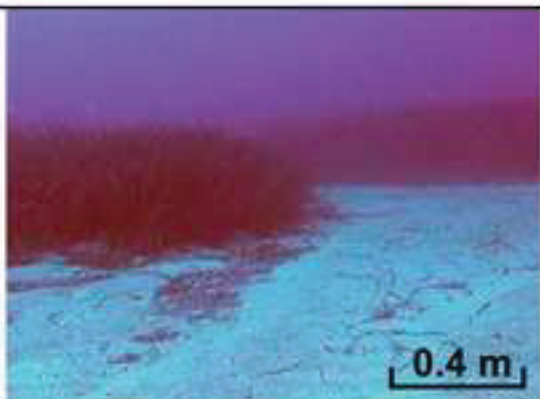

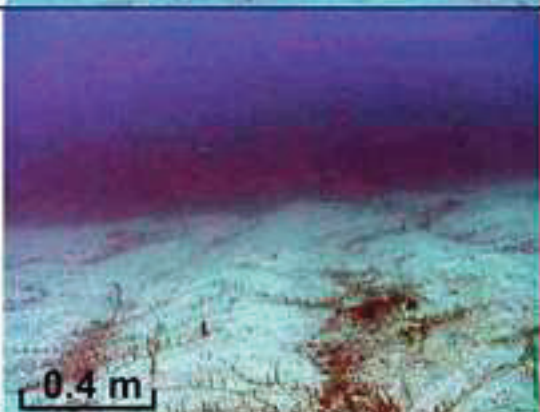

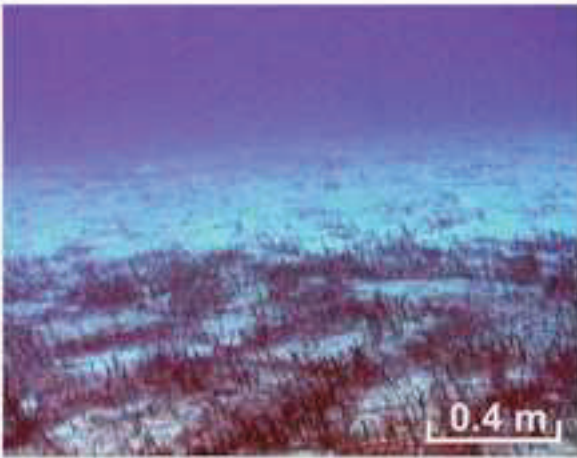
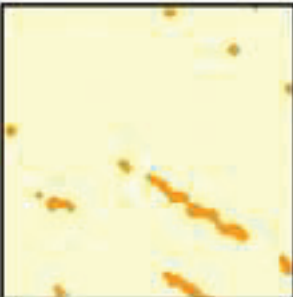
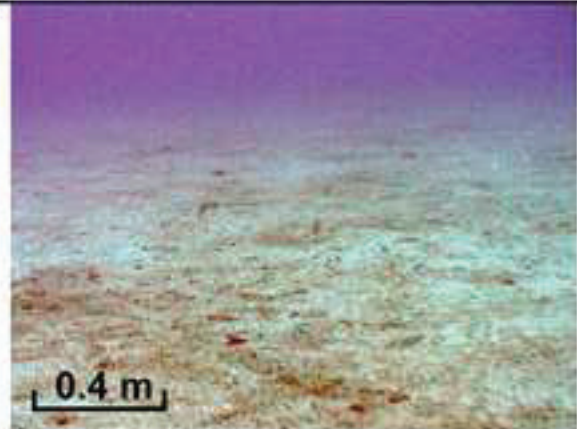
Test site	Predicted seabed composition	Seabed image	Seabed composition
 5	Seagrass on sand, flat	 0.4 m	Superficially medium sand colonised by enclaves of seagrass
 6	Medium sand interrupted by narrow ripples of maerl associated with sand and gravel, flat	 0.2 m	Superficially medium sand interrupted by narrow ripples of maerl associated with sand and gravel; the ripples are colonised by sparse growths of photophilic algae
 7	Seagrass on sand and gravel, flat	 0.4 m	Coarse sand and gravel colonised by patches of seagrass
 8	Maerl interspersed with sand and gravel, flat	 0.4 m	Maerl interspersed with sand and gravel, very sparsely covered by photophilic algae (mainly <i>Caulerpa racemosa</i> )



Figure 9c  
[Click here to download high resolution image](#)

Test site	Predicted seabed composition	Seabed image	Seabed composition
 <p>9</p>	<p>Elongated and curved patches of medium sand draping a maerl associated with sand and gravel, flat</p>	 <p>0.4 m</p>	<p>Elongated and curved patches of medium sand draping a smooth surface of maerl associated with sand and gravel. Photophilic algae (mainly <i>Caulerpa racemosa</i>) occasionally cover patches of maerl associated with sand and gravel.</p>
 <p>10</p>	<p>Maerl associated with sand and gravel, flat</p>	 <p>0.4 m</p>	<p>Maerl associated with sand and gravel</p>